

## Structural and Electrical Characterization of Processable Bis-Silylated Thiophene Oligomers

G. Barbarella,<sup>\*,†</sup> P. Ostojica,<sup>\*,‡</sup> P. Maccagnani,<sup>‡</sup> Olga Pudova,<sup>\*,§</sup> L. Antolini,<sup>\*,||</sup> D. Casarini,<sup>\*,⊥</sup> and A. Bongini<sup>#</sup>

I.Co.C.E.A., L.A.M.E.L., Consiglio Nazionale Ricerche, Via Gobetti 101, 40129 Bologna, Italy, Latvian Institute of Organic Synthesis, Aizkraukles str. 21, Riga, LV-1006, Latvia, Dipartimento di Chimica, Università di Modena, Via Campi 183, 41100 Modena, Italy, Dipartimento di Chimica Organica, Università di Bologna, Via Risorgimento 4, 40110 Bologna, Italy, and Dipartimento di Chimica "G. Ciamician", Università di Bologna, Via Selmi 2, 40126 Bologna, Italy

Received June 12, 1998. Revised Manuscript Received September 10, 1998

A new class of processable, chemically stable, and easily synthesized and purified  $\alpha,\omega$ -bis(dimethyl-*tert*-butylsilyl) oligothiophenes is described. Information on the solid-state properties was obtained by single crystal X-ray diffraction and CPMAS NMR spectroscopy. Molecular packing was characterized by a sandwich-type organization, with the molecular planes between adjacent layers along the stacking direction being exactly parallel. Vacuum-evaporated thin films of the tetramer, pentamer, and hexamer displayed field effect transistor activity, with charge mobilities increasing with the substrate deposition temperatures in the range 28–80 °C. The best FET performance was achieved with the pentamer which was characterized by an on/off ratio  $> 10^3$ , reproducibility, and a device stability in air of months.

The electrical properties of thiophene derivatives are a matter of great current interest since it has been demonstrated that field effect transistors based on these *p*-type semiconductors can achieve charge mobilities and on/off ratios good enough for applications in a variety of devices such as identification cards and flexible displays.<sup>1–4</sup> Processability and chemical stability, needed for solution-phase large area thin film deposition and long-term device performance in air; the low cost of the synthetic procedures; charge mobilities competitive with that of amorphous silicon (0.1–1.0 cm<sup>2</sup>/V.s); and high on/off ratios ( $>10^6$ ) are among the requirements for

industrial application. To our knowledge, no organic semiconductor with all these characteristics is yet available. More research aimed at elucidating charge transport mechanisms and their relation to molecular structure, as well as further research oriented toward device optimization, is still required.

It is now well-established that strong intermolecular ordering and film crystallinity are key features for achieving good carrier mobilities of organic semiconductors at the interface between the gate dielectric and the film.<sup>1–4</sup> Planar molecular conformations and close stacking favor intermolecular  $\pi$ -electron overlap and smaller distances between hopping sites. Organic semiconductors, such as sexithiophene,<sup>1a–d,2a–c</sup> pentacene,<sup>5</sup> and fused thiophene derivatives,<sup>1e,2d,6</sup> give high-quality thin films characterized by high molecular ordering and crystallinity. Also, cast films of conjugated polymers may achieve a high level of order by virtue of self-organization mechanisms and thus display electrical features useful for application in all-plastic devices.<sup>7</sup> The electrical response of all these materials depends to a large extent on the way the device is fabricated and on the way the films are deposited.<sup>1–7</sup>

We are reporting here on the electrical characteristics of a new family of  $\alpha,\omega$ -bis-silylated thiophene oligomers (1–4) which display packing characteristics different from the herringbone arrangement commonly observed in organic molecular solids but similar to that described by Holmes et al. for a fused thiophene derivative.<sup>1e</sup> The

<sup>†</sup> I.Co.C.E.A., Consiglio Nazionale Ricerche.

<sup>‡</sup> L.A.M.E.L., Consiglio Nazionale Ricerche.

<sup>§</sup> Latvian Institute of Organic Synthesis.

<sup>||</sup> Università di Modena.

<sup>⊥</sup> Dipartimento di Chimica Organica, Università di Bologna.

<sup>#</sup> Dipartimento di Chimica "G. Ciamician", Università di Bologna.

(1) (a) Garnier, F.; Yassar, A.; Hajlaoui, R.; Horowitz, G.; Deloffre, F.; Servet, B.; Ries, S.; Alnot, P. *J. Am. Chem. Soc.* **1993**, *115*, 8716. (b) Servet, B.; Horowitz, G.; Ries, S.; Lagorsse, O.; Alnot, P.; Yassar, A.; Deloffre, F.; Srivastava, P.; Hajlaoui, R.; Lang, P.; Garnier, F. *Chem. Mater.* **1994**, *6*, 1809. (c) Garnier, F. *Pure Appl. Chem.* **1996**, *68*, 1455. (d) Garnier, F. *Chem. Phys.* **1998**, *227*, 253. (e) Li, X. C.; Sirringhaus, H.; Garnier, F.; Holmes, A. B.; Moratti, S. C.; Feeder, N.; Clegg, W.; Teat, S. J.; Friend, R. H. *J. Am. Chem. Soc.* **1998**, *120*, 2206. (f) Horowitz, G.; Garnier, F.; Yassar, A.; Hajlaoui, R.; Kouki, F. *Adv. Mater.* **1996**, *8*, 52. (g) Hajlaoui, R.; Horowitz, G.; Garnier, F.; Arche-Brouchet, A.; Laigre, L.; El Kassmi, A.; Demanze, F.; Kouki, F. *Adv. Mater.* **1997**, *9*, 389. (h) Garnier, F.; Hajlaoui, R.; Yassar, A.; Srivastava, P. *Science* **1994**, *265*, 1684.

(2) (a) Torsi, L.; Dodalabapur, A.; Rotheberg, L. J.; Fung, A. W. P.; Katz, H. E. *Science* **1996**, *272*, 1462. (b) Lovinger, A. J.; Rothberg, L. J. *J. Mater. Res.* **1996**, *11*, 1581. (c) Katz, H. E. *J. Mater. Chem.* **1997**, *7*, 369. (d) Laquindanum, J. G.; Katz, H. E.; Lovinger, A. J. *J. Am. Chem. Soc.* **1998**, *120*, 664. (e) Katz, H. E.; Lovinger, A. J.; Laquindanum, J. G. *Chem. Mater.* **1998**, *10*, 457. (f) Katz, H. E.; Laquindanum, J. G.; Lovinger, A. J. *Chem. Mater.* **1998**, *10*, 633.

(3) Horowitz, G. *Adv. Mater.* **1998**, *10*, 365.

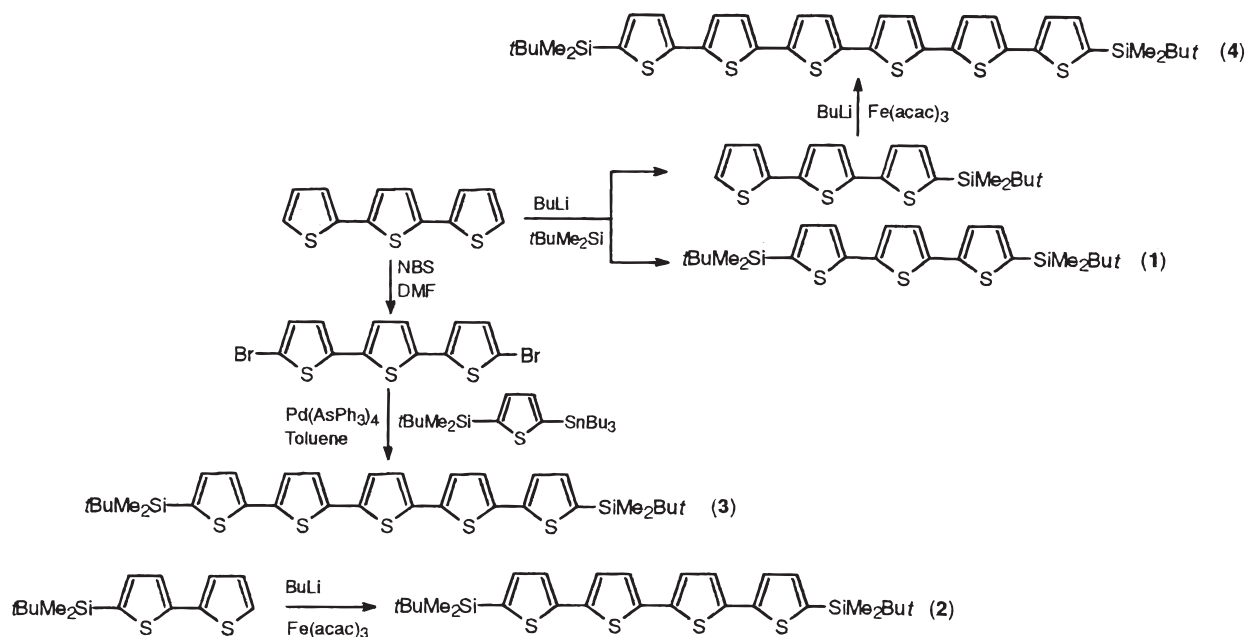
(4) Brown, A. R.; Jarret, C. P.; de Leeuw, D. M.; Matters, M. *Synth. Met.* **1997**, *88*, 37.

(5) Jackson, T. *Science* **1996**, *273*, 879.

(6) Sirringhaus, H.; Friend, R. H.; Li, X. C.; Moratti, S. C.; Holmes, A. B.; Feeder, N. *Appl. Phys. Lett.* **1997**, *71*, 3871.

(7) Bao, Z.; Feng, Y.; Dodabalapur, A.; Raju, V. R.; Lovinger, A. J. *Chem. Mater.* **1998**, *9*, 11299.

## Scheme 1. Synthetic Pattern followed for the Preparation of Compounds 1–4



chemical structure and the synthetic pattern followed for the preparation of compounds **1–4**, starting from commercially available bi- and terthiophene, are given in Scheme 1.

## Results

**Synthesis of Materials.** Scheme 1 gives the synthetic pattern followed for the preparation of compounds **1** (SiTTTTSi) and **3** and **4** (SiTTTTTTSi and SiTTTTTTTSi). The synthesis of tetramer **2** (SiTTTTTSi) through oxidative coupling of 5-(dimethyl-*tert*-butyl)-5'-lithio-2,2'-bithiophene with Fe(acac)<sub>3</sub> has already been reported.<sup>8a</sup>

The synthetic procedures reported in Scheme 1 are straightforward and involve mainly routine bromination and lithiation steps. The  $\alpha,\omega$ -dibromo derivative of terthiophene was obtained quantitatively from the commercial precursor using N-bromosuccinimide in dimethylformamide.<sup>9</sup> The dibromo derivative was then coupled to 2-(dimethyl-*tert*-butylsilyl)thiophene<sup>8a</sup> using Pd(AsPh<sub>3</sub>)<sub>4</sub> generated in situ as the catalyst<sup>8b</sup> to afford pentamer **3** in 57% yield (after purification by silica gel chromatography). All compounds were soluble in common organic solvents and were purified by silica gel chromatography.

For all compounds the  $\lambda_{\max}$  values in chloroform were red-shifted with respect to those of the unsubstituted counterparts (SiTTTTSi = 370 nm, TTT = 352 nm; SiTTTTTTSi = 412 nm, TTTT = 390 nm; SiTTTTTTTSi = 420 nm, TTTTT = 416 nm; SiTTTTTTTTSi = 440 nm, TTTTTT = 432 nm).

Single crystals suitable for X-ray structure determinations were obtained for compounds **1** and **2**, from

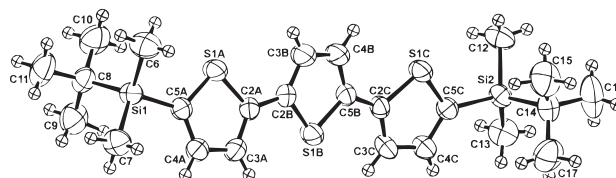


**Figure 1.** Molecular structure of trimer **1** with atom numbering scheme. Selected bond distances (Å with esd's in parentheses): S1A–C2A, 1.716(2); S1A–C5A, 1.721(2); S1B–C2B, 1.719(2); S1B–C5B, 1.720(2); S1C–C2C, 1.714(2); S1C–C5C, 1.724(2); C2A–C2B, 1.458(3); C5B–C2C, 1.462(3); C5A–Si1, 1.868(2); C5C–Si2, 1.865(2).

chloroform solutions, whereas compounds **3** and **4** were obtained in the form of microcrystalline powders.

**Single-Crystal X-ray Structure Determinations.** Compound **1** is air stable and yields colorless crystals: space group  $P\bar{1}$ ,  $a = 6.607(1)$  Å,  $b = 12.641(2)$  Å,  $c = 17.514(2)$  Å,  $\alpha = 71.08(1)^\circ$ ,  $\beta = 89.79(1)^\circ$ ,  $\gamma = 87.95(1)^\circ$ ,  $V = 1382.8(4)$  Å<sup>3</sup>,  $\rho_{\text{calc}} = 1.145$  Mg/m<sup>3</sup> for  $Z = 2$ . Compound **2** is air stable and gives light green crystals: space group  $P\bar{1}$ ,  $a = 6.577(1)$  Å,  $b = 6.578(1)$  Å,  $c = 17.853(4)$  Å,  $\alpha = 85.24(1)^\circ$ ,  $\beta = 81.47(1)^\circ$ ,  $\gamma = 77.25(1)^\circ$ ,  $V = 744.0(2)$  Å<sup>3</sup>,  $\rho_{\text{calc}} = 1.248$  Mg/m<sup>3</sup> for  $Z = 1$ .

Drawings of the molecular structure of compounds **1** and **2** are presented in Figures 1 and 3, respectively, along with atom numbering schemes, while stereoviews of the molecular packing are presented in Figures 2 and 4.

The molecular dimensions of the two compounds are very similar. Common features are a quasiplanar anti conformation, the same antiperiplanar orientation of the silyl substituents, and a quite similar sandwich-type packing mode.

The asymmetric unit of **1** contains one molecule characterized by S–C $_{\alpha}$ –C $_{\alpha}$ –S torsion angles of  $-165.0(1)^\circ$  and  $-167.0(1)^\circ$ . The mean plane through the atoms of the central ring makes dihedral angles of  $13.2(1)^\circ$  and  $11.3(1)^\circ$  with those defined by the outer rings. The molecular conformation of **1** is very close to those

(8) (a) Barbarella, G.; Pudova, O.; Arbizzani, C.; Mastragostino, M.; Bongini, A. *J. Org. Chem.* **1998**, *63*, 1742. (b) Barbarella, G.; Zambianchi, M.; Sotgiu, G.; Bongini, A. *Tetrahedron* **1997**, *53*, 9401. (c) Barbarella, G.; Casarini, D.; Zambianchi, M.; Favaretto, L.; Rossini, S. *Adv. Mater.* **1996**, *8*, 69.

(9) Bäuerle, P.; Würthner, F.; Götz, G.; Effenberger, F. *Synthesis* **1993**, 1099.

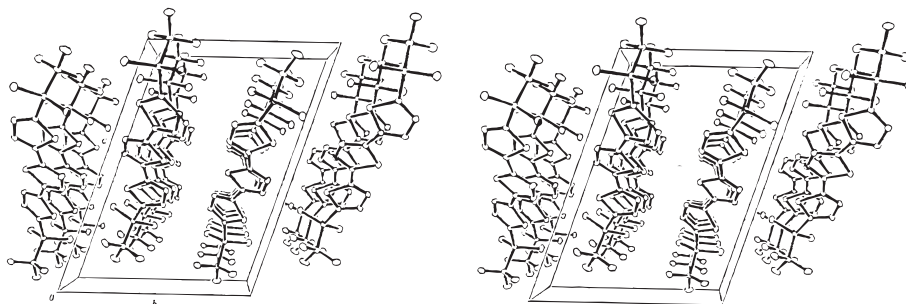


**Figure 2.** Stereoview of the molecular packing of trimer **1**.

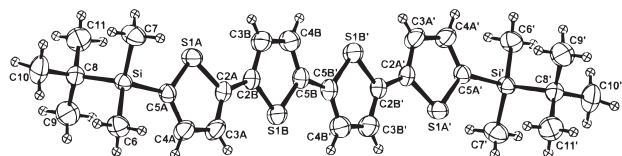


**Figure 3.** Molecular structure of tetramer **2** with atom numbering scheme. Primed atoms are related to unprimed ones by an inversion center at the midpoint of the C5–C5' bond. Selected bond distances (Å with esd's in parentheses): S1A–C2A, 1.719(2); S1A–C5A, 1.725(2); S1B–C2B, 1.725(3); S1B–C5B, 1.731(3); C2A–C2B, 1.458(4); C5B–C5B', 1.451(5); C5A–Si, 1.865(3).

observed for the two crystallographically independent molecules of the unsubstituted terthiophene and that reported for the trimethyl-substituted analogue.<sup>10,11a</sup>

The molecule of **2** is located on a crystallographic center of symmetry at the midpoint of the central interring bond. The inner rings are therefore exactly coplanar and their S atoms anti to each other. The outer rings are slightly twisted with respect to the inner ones [9.1(1)°], their S atoms being transoid about the ring junction [–169.8(1)°]. It is of interest to note that a centrosymmetric, quasiplanar, and all-trans conformation was previously observed for the  $\alpha$ -quaterthiophene and for its  $\alpha,\omega$ -dimethyl- and 4,4',3'',4'''-tetramethyl substituted analogues.<sup>11b,12,13</sup> These latter compounds exhibit only smaller tilt angles between inner and outer rings.

There are no significant differences between corresponding bond distances and angles of **1** and **2**, and their values compare very well with those reported for the above cited compounds and other methyl-substituted quaterthiophenes of known structure.<sup>11c</sup> Hence, the bulky silyl substituents do not appear to exert any effect on the preferred conformation of  $\alpha$ -conjugated ter- and quaterthiophenyl derivatives.

The presence of bulky substituents at the terminal positions of **1** and **2** seems to play an important role in determining the molecular packing. The molecules of planar or quasiplanar oligothiophenes are usually arranged in the crystal to form a herringbone packing

motif, with herringbone angles which normally span between 60 and 70°. <sup>14–16</sup> In the present compounds, the presence of the silyl groups, which lie above and below the thienyl mean planes, leads to a centric triclinic cell containing one or two molecules and to a sandwich-type molecular packing. It is worth noting that the same molecular arrangement in oligothiophene derivatives was previously observed only for the triclinic, more tilted, phase of the polymorphic tetrakis(methylsulfonyl)-2,2':5',2'':5'',2''':5''',2''''-quaterthiophene.<sup>11d,e</sup> Nevertheless, the molecular packing of both compounds does not contain any van der Waals contact significantly less than 3.60 Å. The shortest S...S intermolecular separations, a parameter of great interest from the point of view of the crystal conductivity, are 4.627(2) and 4.200(2) Å in **1** and **2**, respectively. It may also be of interest to note that all atoms of both compounds, including those belonging to silyl groups, display unusually low crystallographic thermal motion parameters, indicative of a quite rigid molecular framework. It is likely that this effect is due to the bulky silyl substituents.

**<sup>13</sup>C and <sup>29</sup>Si CPMAS NMR Spectroscopy.** With the purpose of gaining information on the solid-state organization properties of pentamer **3**, which showed good FET performance (see below), we carried out <sup>13</sup>C and <sup>29</sup>Si CPMAS NMR<sup>17</sup> experiments on microcrystalline powders of this compound and compared the results to those of compounds **1** and **2**. We have already shown that this technique gives a great deal of information on the solid-state characteristics of oligothiophenes.<sup>8c</sup>

The <sup>13</sup>C and <sup>29</sup>Si CPMAS chemical shifts of compounds **1–3** are reported in Table 1.

Carbon chemical shifts were assigned by comparison to solution data and were confirmed by nonquaternary suppression (CP–NQS) experiments that select only the quaternary and mobile carbons (the latter generally being methyl groups).<sup>17d</sup>

As in the case of unsubstituted oligothiophenes,<sup>8c</sup> the spectra of **2**, with an even number of thiophene units, and those of **1** and **3**, with an odd number of thiophene units, were remarkably different. In **2**, the number of carbon signals was half the number of carbons in the molecule (only four quaternary carbons and four CHs of the thiophene rings and single signals for the

(10) Van Bolhuis, F.; Wynberg, H.; Havinga, E. E.; Meijer, E. W.; Staring, E. G. *J. Synth. Met.* **1989**, *30*, 381.

(11) (a) Barbarella, G.; Zambianchi, M.; Bongini, A.; Antolini, L. *Adv. Mater.* **1994**, *6*, 561. (b) *Adv. Mater.* **1992**, *4*, 282. (c) *Adv. Mater.* **1993**, *5*, 834. (d) Barbarella, G.; Zambianchi, M.; Di Toro, R.; Colonna, M.; Antolini, L.; Bongini, A. *Adv. Mater.* **1996**, *8*, 327. (e) Barbarella, G.; Zambianchi, M.; Fresno Marimon, M.; Antolini, L.; Bongini, A. *Adv. Mater.* **1997**, *9*, 484.

(12) (a) Antolini, L.; Horowitz, G.; Kouki, F.; Garnier, F. *Adv. Mater.* **1998**, *10*, 385. (b) Siegrist, T.; Kloc, C.; Laudise, R. A.; Katz, H. E.; Haddon, R. C. *Adv. Mater.* **1998**, *10*, 379.

(13) Hotta, S.; Waragai, K. *J. Mater. Chem.* **1991**, *1*, 835.

(14) Gavezzotti, A.; Filippini, G. *Synth. Met.* **1991**, *40*, 257.

(15) Porzio, W.; Destri, S.; Mascherpa, M.; Bruckner, S. *Acta Polym.* **1993**, *44*, 266.

(16) Lovinger, A. J.; Davis, D. D.; Dodabalapur, A.; Katz, H. E. *Chem. Mater.* **1996**, *8*, 2886.

(17) (a) Voelkel, R. *Angew. Chem., Int. Ed. Engl.* **1988**, *27*, 1468. (b) Yannoni, C. S. *Acc. Chem. Res.* **1982**, *15*, 201. (c) Yannoni, C. S. *Acc. Chem. Res.* **1982**, *15*, 208. (d) Opella, S. J.; Frey, M. H. *J. Am. Chem. Soc.* **1979**, *101*, 5854.



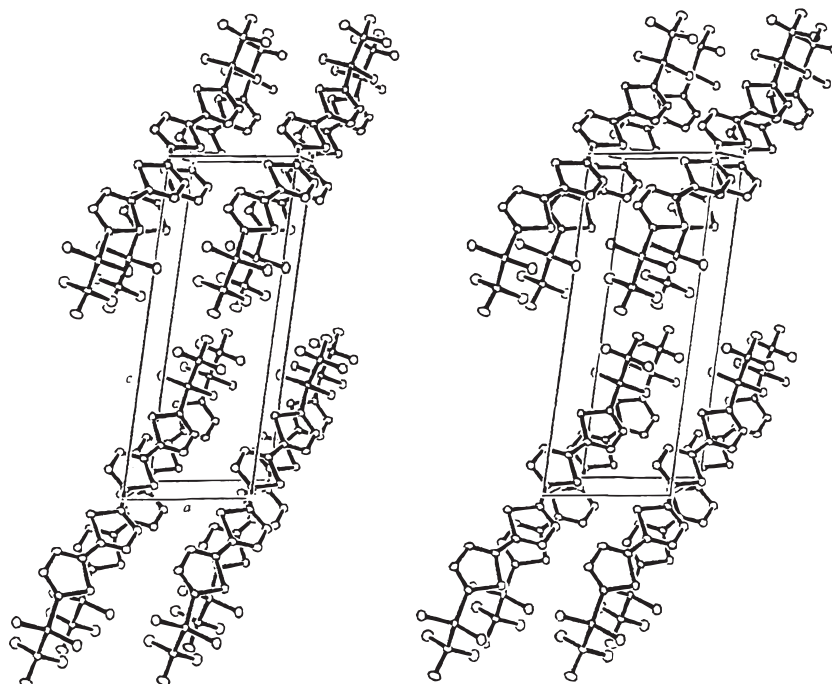


Figure 4. Stereoview of the molecular packing of tetramer **2**.

Table 1.  $^{13}\text{C}$  and  $^{29}\text{Si}$  CPMAS NMR Chemical Shifts<sup>a</sup> of Compounds **1–3**

compd	Si	<i>t</i> -Bu		thiophene		$(\text{CH}_3)_2\text{Si}$
		C	CH <sub>3</sub>	CH	C	
<b>1</b>	0.91(19.0) <sup>b</sup>	17.6(2) <sup>c</sup>	26.4(3) <sup>c</sup>	125.0(3) <sup>c</sup>	135.7(4) <sup>c</sup>	-6.7, -3.4
			26.8(3) <sup>c</sup>	126.3(4) <sup>c</sup>	143.1	-5.9, -3.0
			137.1	144.0		
<b>2</b>	1.18(12.0) <sup>b</sup>	18.1(2) <sup>c</sup>	27.8(6) <sup>c</sup>	123.6	135.2	-5.6, -3.3
				125.4	135.7	
				125.6	137.2	
				137.7	143.4	
				138.3		
<b>3</b>	0.94(12.0) <sup>b</sup> 1.43(12.0) <sup>b</sup>	17.6	26.4(6) <sup>c</sup>	124.5(2) <sup>c</sup>	135.3	-6.7, -3.8
				125.9(6) <sup>c</sup>	136.2(5) <sup>c</sup>	-5.9, -2.3
				137.6(2) <sup>c</sup>	143.6(2) <sup>c</sup>	

<sup>a</sup> Chemical shifts with respect to TMS. <sup>b</sup> Linewidth in Hertz. <sup>c</sup> Estimated overall intensity.

Table 2. Field-Effect Mobilities of **2–4** as a Function of Substrate Deposition Temperature

compd	temp (°C)	mobility (cm <sup>2</sup> /V s)
<b>2</b>	28, 70,	$2 \times 10^{-7}$ , $8 \times 10^{-6}$
	90	no FET activity
<b>3</b>	28, 60, 70, 80,	$1 \times 10^{-5}$ , $5 \times 10^{-5}$ , $3 \times 10^{-4}$ , $2 \times 10^{-4}$ ,
	90	no FET activity
<b>4</b>	28, 60,	$1 \times 10^{-5}$ , $4 \times 10^{-5}$ ,
	90	no FET activity

quaternary and methyl carbons of the *t*-Bu groups). This indicates that in the microcrystalline powder of **2** the asymmetric unit corresponds only to half of the molecule; i.e. there is a symmetry element which makes the two halves of the molecule equivalent. Furthermore, the methyls bonded to Si, which show two sharp peaks at -5.6 and -3.3 ppm (see Figure 5b) instead of a single signal, indicate that the molecular plane (the one containing the thiophene rings) does not bisect the angle between the two geminal methyls making them diastereotopic. Thus, the element of symmetry that makes the two half-molecules equivalent must be centered

between the inner rings. These results agree fully with the packing characteristics observed by the single-crystal X-ray determinations of **2**.

Contrary to what is observed for compound **2**, for **1** and **3** the geminal methyls bonded to the silicon atom yielded four (instead of two) signals (see Figure 5b), indicating that the two halves of the molecule are not equivalent. As shown in Table 1, splitting of the signals was also detected for the methyls of the *t*-Bu group and for the quaternary and CH carbons of the aromatic skeleton in the regions around 143 and 137 ppm.

Further  $^{29}\text{Si}$  CPMAS experiments also showed a different number of signals for compounds **2** and **3**. Indeed, two sharp  $^{29}\text{Si}$  lines separated by 29 Hz were detected for **3**, whereas for **2** only a single sharp line was detected, coinciding with the midpoint of the separation observed in **3** (see Figure 5a). For **1**, a single line was detected that is much broader than that observed for **2** (19 against 12 Hz) arising from the overlapping of two different signals with a very small peak separation.

From these data we can unambiguously conclude that the packing characteristics of pentamer **3** are the same as those of trimer **1**.

**Field Effect Transistors.** Thin film transistors were fabricated by vacuum evaporation of compounds **2–4** on test patterns according to the ways described in ref 18a. The source-drain characteristics of the transistors fabricated with the pentamer SiTTTTTSi (**3**) deposited at substrate temperatures of 28, 60, and 80 °C are reported in Figure 6a–c. The transistors presented well-defined saturation regimes and currents which increased with the increasing of the substrate temperature during the deposition, as observed in the

(18) (a) Ostojia, P.; Guerri, S.; Improta, M.; Zabberoni, P.; Danieli, R.; Rossini, S.; Taliani, C.; Zamboni, R. *Adv. Mater. Opt. Electron.* **1992**, *1*, 127. (b) Ostojia, P.; Guerri, S.; Rossini, S.; Servidori, M.; Taliani, C.; Zamboni, R. *Synth. Met.* **1993**, *54*, 447.

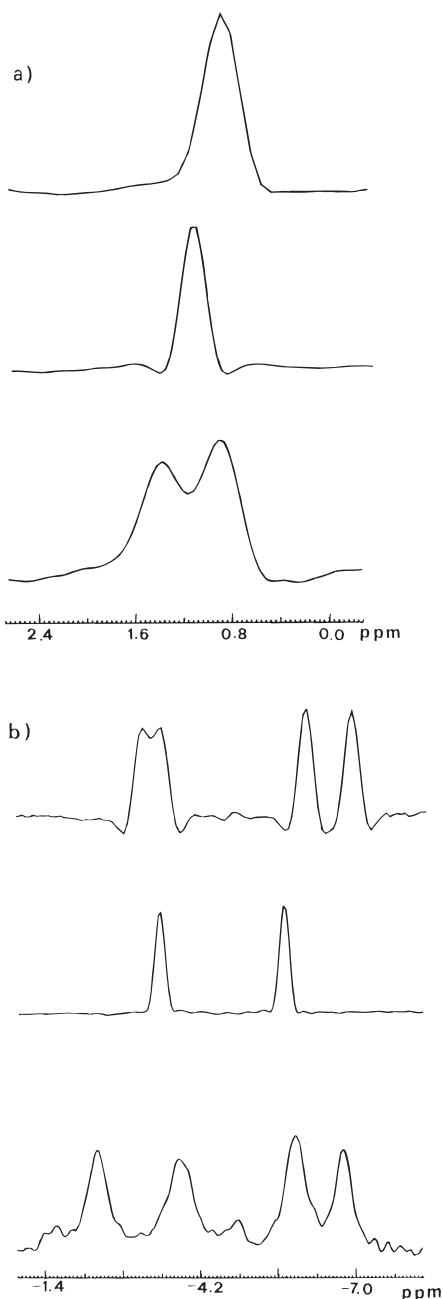


**Figure 5.**  $^{29}\text{Si}$  (a) and  $^{13}\text{C}$  (b) CPMAS NMR spectra of compounds **1–3**: (Top) terthiophene **1**, (middle) quaterthiophene **2**, (bottom) quinquethiophene **3**.

case of other oligothiophene-based transistors.<sup>19,2d,e</sup> The useful range of temperature was 28–80 °C. For films of all oligomers deposited at 90 °C, no transistor effect was detected. Indeed, at this temperature the films presented a different morphology, with many fractures which implied a loss of continuity of the film itself.

As the currents increase with the increasing of the negative gate voltages, it can be concluded that compounds **2–4** are p-type semiconductor materials. Measurements performed on the same devices after many weeks revealed good reproducibility, thus demonstrating

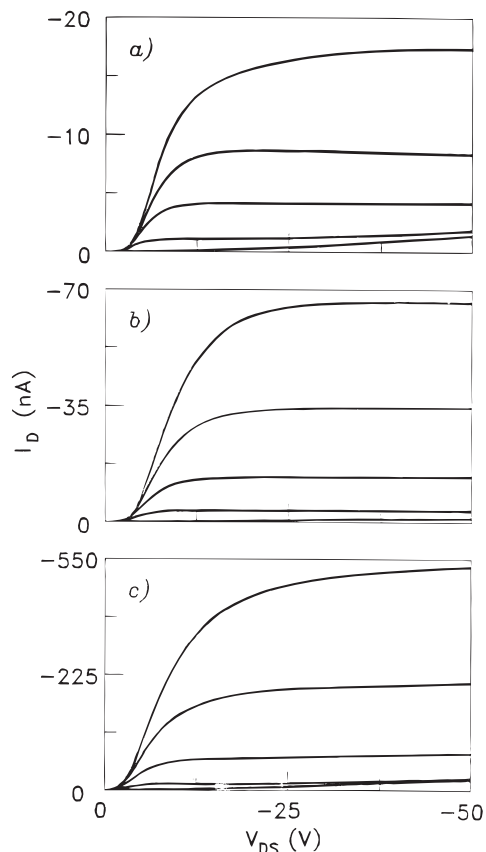


**Figure 6.** Source-drain characteristics of the thin film transistors fabricated with pentamer **3** deposited at substrate temperatures of 28 (a), 60 (b), and 80 °C (c). In each figure the lowest curve refers to a gate voltage  $V_G = 0$  V and the highest to a gate voltage  $V_G = -40$  V.

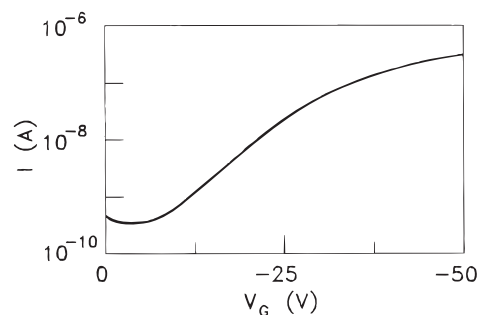


**Figure 7.** Transfer characteristic of the FET corresponding to Figure 6c.

the good stability of the films in air. This was particularly true for compound **3**, since the characteristics of the FETs based on this compound were found to be the same after 5 months.

Field-effect mobilities of **2–4** as a function of substrate deposition temperature are reported in Table 2.

Charge mobilities ( $\mu$ ) were calculated by using eq 1:

$$g_m = (\delta I_d / \delta V_g) V_{d=0} = W/L(C_i \mu V_d) \quad (1)$$

where  $g_m$  is the transconductance,  $C_i$  is the insulator capacitance per unit area,  $I_d$  is the drain current,  $V_d$  and  $V_g$  are the source-drain and the source-gate voltages,  $W$  is the channel width, and  $L$  is the channel length.

(19) Servet, B.; Horowitz, G.; Ries, S.; Lagorsse, O.; Alnot, P.; Yassar, A.; Deloffre, F.; Srivastava, P.; Hajlaoui, R.; Lang, P.; Garnier, F. *Chem. Mater.* **1994**, *6*, 1809.

The transfer characteristic of the FET corresponding to Figure 6c is reported in Figure 7, showing an on/off ratio  $> 10^3$ .

### Discussion

Attractive features of the compounds described here are the ease of synthesis and purification and the reproducibility and stability of the FET devices in air.

Furthermore, the highly ordered stacked molecular arrangement which, according to X-rays and  $^{13}\text{C}$  CP-MAS NMR, is achieved by these compounds in the crystalline state (and which may be considered as being the upper limit in terms of molecular organization) is promising with respect to the possibility of obtaining a high level of molecular ordering also in the thin films employed for FET devices.

Since stacked structures favor high mobilities,<sup>1e,2d,6</sup> we can reasonably expect the intrinsic carrier mobilities of our bis-silylated oligothiophenes to be higher than those reported in Table 1, provided films with this type of molecular organization are obtained. Thus, further work aimed, in particular, at establishing the structural order of oligomer molecules in the thin films (see, for example, ref 1b) is required and we are currently investigating in this direction.

It is known that the quality of the films used for FET devices is related not only to the characteristics of the organic compounds but also to the methods of film preparation.<sup>1-6</sup> The films used in this study were obtained by vacuum evaporation using a very low deposition rate, but the solubility of compounds 2-4 will allow solution-phase deposition procedures to also be employed. The level of molecular organization attained by solution-phase deposition can indeed also be very high, as shown for example by the data reported in ref 2f. Thus, the possibility of obtaining more efficient devices using different deposition procedures for compounds 2-4 will also be tested.

Although the charge mobilities that have been measured for oligothiophenes 2-4 (Table 2) are not as high as those reported recently for other thiophene oligomers,<sup>1-4</sup> the quality of the devices obtained (particularly for pentamer 3) is rather good, with well-defined saturation regimes and easily achievable on/off ratios  $> 10^3$  (Figures 6 and 7). More importantly, there is much room to improve the device performance by using different test patterns, with lower contact resistance.

The increase of charge mobilities observed on increasing the substrate deposition temperature indicates that there is a progressive reordering of the film structure of 2-4 at higher temperatures. The useful temperature range is 30-80 °C, since when the substrate is heated to 90 °C the films of all compounds present several fractures and no more transistor effect is observed. The increase of charge mobility observed on heating the substrate is quite substantial (30-40 times; see Table 2) and much larger than that reported so far for other oligothiophenes such as unsubstituted sexithiophene,<sup>19</sup> antradithiophenes,<sup>2d</sup> or dihexylquaterthiophenes.<sup>2e</sup>

According to X-ray and CP-MAS NMR data, the solid-state organization of our bis-silylated derivatives gives rise to a rather rigid molecular network. Indeed, the geminal methyl groups of the antiperiplanar silyl substituents of a given molecule fit perfectly with the

staggered methyls of the adjacent *tert*-butyl group, the molecular conformation is nearly planar, and there is a strict piling up of all molecules in parallel planes. Given these characteristics, it is difficult to predict the nature of the processes promoted by the heating of the substrate, in particular whether an increase of film crystallinity or a different and more favorable molecular orientation with respect to the substrate are involved. Nevertheless, we believe that the trend observed for the charge mobilities of 2-4 on heating the substrate is a further indication that carrier mobilities greater than those reported in Table 2 could be attained for these compounds.

As shown in Table 2, the charge mobilities measured for pentamer 3 are the same as those obtained with hexamer 4 (which is more difficult to synthesize and purify). This result seems in agreement with the hypothesis made by Garnier et al., according to which in thiophene oligomers, as in other organic molecules, charge mobility should be independent of the length of the conjugated system.<sup>1g</sup> On the other hand, this ideal behavior would require the absence of any polymorphism (to be sure that oligomers of different length and symmetry are packed in a similar way in thin films), while for unsubstituted oligothiophenes there is large experimental evidence that this is not necessarily the case.<sup>1b,12</sup> The presence of substituents should restrict the number of possible polymorphs and we notice indeed that, so far, no evidence has been provided of polymorphism on oligothiophenes substituted at the end positions.

In conclusion, we believe that, owing to their peculiar solid-state organization properties, the bis-silylated thiophene oligomers described in this paper (soluble in most organic solvents and easy to synthesize and purify) are good models for investigating the relationship between molecular structure and electrical properties of thiophene oligomers. We are currently modifying the geometry of our FET device and testing different film deposition methods to ascertain whether the charge mobility of our compounds can be increased to the level reported for other thiophene-based organic molecules.

### Experimental Section

**Synthesis of Materials.** Iron(III) acetylacetonate, 2,2'-bithiophene, 2,2':5':2''-terthiophene, Pd<sub>2</sub>dba<sub>3</sub>, AsPh<sub>3</sub>, BuLi, and Me<sub>3</sub>SnCl were purchased from Aldrich. All solvents used in reactions and chromatographies were dried by standard procedures. Flash chromatographies were carried out using silica gel (230-400 mesh ASTM) and analytical thin layer chromatographies (TLCs) using 0.2 mm silica gel plates (Merck). The visualization for TLC was accomplished by UV light. The synthesis of compounds 1 and 2 has already been described.<sup>8a</sup>

5,5''''-bis(dimethyl-*tert*-butylsilyl)-2,2':5',2'':5''',2''':5''''-quinquethiophene, 3. To a 20 mL toluene solution of Pd(AsPh<sub>3</sub>)<sub>4</sub> generated in situ<sup>8b</sup> were added 0.406 g (1.0 mmol) of 5,5''-dibromo-2,5:5',2''-terthiophene<sup>9</sup> and 0.972 g (2.0 mmol) of 2-(dimethyl-*tert*-butylsilyl)-5-(tributylstannyl)thiophene.<sup>8a</sup> After heating at reflux for 12 h, the reaction mixture was hydrolyzed with a saturated solution of NH<sub>4</sub>Cl and extracted with CH<sub>2</sub>Cl<sub>2</sub>, the organic phase was dried over MgSO<sub>4</sub>, concentrated, filtered on silica gel, and evaporated. The residue was washed with ethyl ether and 0.364 g (57% yield) of an orange microcrystalline solid, mp 211-212 °C, was recovered. MS: *m/e* 640 (M<sup>+</sup>).  $\lambda_{\text{max}}(\text{CHCl}_3) = 420 \text{ nm}$ . <sup>1</sup>H NMR (CDCl<sub>3</sub>, TMS/ppm): 7.24 (d, *J* = 3.6 Hz, 2H), 7.14 (d, *J*

= 3.6 Hz, 2H), 7.10 (d,  $J = 3.7$  Hz, 2H), 7.08 (d,  $J = 3.7$  Hz, 2H), 7.07 (s, 2H), 0.95 (s, 18H), 0.31 (s, 12H).  $^{13}\text{C}$  NMR ( $\text{CDCl}_3$ , TMS/ppm): 142.9, 138.1, 137.2, 136.6, 125.6, 125.2, 125.1, 125.0, 27.1, 17.6, -4.2. Anal. Calcd for  $\text{C}_{32}\text{H}_{40}\text{S}_6\text{Si}_2$ : C, 59.95; H, 6.29. Found C, 59.83; H, 6.27.

5,5''''-Bis(dimethyl-*tert*-butylsilyl)-2,2':5',2'':5'',2''':5''',2''''':5''''''-sexithiophene, **4**. To a solution of 0.40 g (1.1 mmol) of 5-(dimethyl-*tert*-butylsilyl)-2,2':5',2''-terthiophene<sup>8a</sup> was added dropwise 0.44 mL (1.1 mmol) of a 2.5 M solution of BuLi in hexane. After 30 min, 0.39 g (1.1 mmol) of  $\text{Fe}(\text{acac})_3$  was added and the mixture stirred for 3 h at room temperature. Then 30 mL of a 3 M solution of HCl was added, the reaction mixture extracted with  $\text{CH}_2\text{Cl}_2$ , the organic layer washed with brine, dried over  $\text{MgSO}_4$ , and evaporated. The residue was washed with ethyl ether, and 0.23 g (58% yield) of **4** as a dark red microcrystalline compound, mp 244–245 °C, was recovered. MS:  $m/e$  722 ( $\text{M}^+$ );  $\lambda_{\text{max}}(\text{CHCl}_3) = 440$  nm.  $^1\text{H}$  NMR ( $\text{CDCl}_3$ , TMS/ppm): 7.21 (d,  $J = 3.4$  Hz, 2H), 7.10 (d,  $J = 3.4$  Hz, 2H), 7.06 (s, 8H), 0.94 (s, 18H), 0.30 (s, 12H). Anal. Calcd for  $\text{C}_{36}\text{H}_{42}\text{S}_6\text{Si}_2$ : C, 59.78; H, 5.85. Found: C, 59.67; H, 5.94.

**X-ray Measurements.** *Compound 1*: Crystal dimensions,  $0.40 \times 0.25 \times 0.25$  mm; Enraf-Nonius CAD4 diffractometer, graphite-monochromated Mo  $K\alpha$  radiation, room temperature. 6630 reflections collected in the range  $2^\circ = \theta = 27^\circ$ ; 6023 symmetry-independent reflections with  $I \geq 2\sigma(I)$  used, without absorption correction ( $\mu = 0.364 \text{ mm}^{-1}$ ), in the structure solution (direct methods: SHELX-86) and least-squares refinement (SHELX-93) of 373 parameters. All non-hydrogen atoms were refined anisotropically, and H atoms were located in  $\Delta F$  maps, isotropically (with two common temperature factors). Final  $R$  and  $wR^2$  values were 0.0386 and 0.1052, respectively.

*Compound 2*: Crystal dimensions,  $0.33 \times 0.28 \times 0.20$  mm; Siemens P4RA-M18X diffractometer, graphite-monochromated Mo  $K\alpha$  radiation (52 kV, 90 mA), room temperature. 3702 reflections collected in the range  $2^\circ = \theta = 26^\circ$ ; 2909 symmetry-independent reflections with  $I \geq 2\sigma(I)$  used, without absorption correction ( $\mu = 0.416 \text{ mm}^{-1}$ ), in the structure solution (direct methods: SHELX-86) and least-squares refinement (SHELX-93) of 212 parameters. All non-hydrogen atoms were refined anisotropically, and H atoms were located in  $\Delta F$  maps, isotropically (with one common temperature factor). Final  $R$  and  $wR^2$  values were 0.0507 and 0.1331, respectively.

Further details of the crystal structure determinations are available on request from the Cambridge Crystallographic Data Centre, University Chemical Laboratory, Lensfield Road, Cambridge CB2 1EW, UK, on quoting the names of the authors and the journal citation.

**$^{13}\text{C}$  and  $^{29}\text{Si}$  CP-MAS NMR.**  $^{13}\text{C}$  and  $^{29}\text{Si}$  CP-MAS NMR spectra were obtained with a Bruker CXP-300 spectrometer operating at 75.45 and 59.60 MHz, respectively. The samples were packed into a 7 mm rotor that was spun at the magic angle with a spinning rate in the range of 3.5–4.3 kHz. For  $^{13}\text{C}$  CP-MAS experiments the  $90^\circ$   $^1\text{H}$  pulse duration was 5  $\mu\text{s}$ ,

which was also the value for  $^{13}\text{C}$  as required by the Hartmann–Hahn conditions. The contact time was 1 ms, the recycle delay was 8s. For  $^{29}\text{Si}$  CP-MAS experiments the  $90^\circ$   $^{29}\text{Si}$  pulse duration was 3.5  $\mu\text{s}$ , the contact time 2 ms and the recycle delay 10s. The number of transients were varied as required to achieve a good signal-to-noise ratio. The chemical shifts were calibrated by replacement, for the  $^{13}\text{C}$  spectra with respect to the lower frequency signal of adamantane (quoted as 29.4 ppm with respect to TMS) and for  $^{29}\text{Si}$  with respect to TMS itself.  $^{13}\text{C}$  as well as  $^{29}\text{Si}$  chemical shifts were reported with respect to TMS (0 ppm).

**Field Effect Transistors.** The organic TFTs were fabricated by using silicon single-crystal wafers (p-type, 100  $\Omega\cdot\text{cm}$ , (100) oriented, 300  $\mu\text{m}$  thick) as substrates. Phosphorus was thermally diffused at the surface, and this heavily doped layer (about  $10^{19} \text{ cm}^{-3}$ ) was used as distributed gate, on which a dielectric layer of 250 nm of  $\text{SiO}_2$  was grown by thermal oxidation. After a first photolithographic step for opening the via for the gate contact, a double layer of 30 nm of Ti (which acts as an adhesion layer) and 170 nm of Au (which is known to give an ohmic contact to p-type oligomers) was successively evaporated under the same vacuum cycle. Thereafter an interdigitated structure of the source-drain contacts was photolithographically delineated, determining a channel width of 1.2  $\mu\text{m}$ , with a channel length of 10  $\mu\text{m}$ . This kind of structure minimizes the contact area (thus avoiding gate to source-drain leakage currents) and yields higher source-drain currents.

After scribing, every chip was washed in an ultrasonic bath with a 1:1 solution of  $\text{H}_2\text{SO}_4 + \text{H}_2\text{O}_2$  for 2 min, followed by a dip of 2 min in deionized water and, as a final step, a dip of 10 s in a solution 1:100 of HF +  $\text{H}_2\text{O}$ . Thin layers (50 nm thick) of oligomers were deposited on the channel region by vacuum evaporation through a metal mask. The vacuum was kept at  $1 \times 10^{-6}$  mbar and the evaporation temperature was between 200 and 300 °C (the lowest for tetramer **2** and the highest for hexamer **4**). During the evaporation, performed at a rate of 0.1–0.5 nm/s, the substrate was kept at ambient temperature (28 °C) or at higher temperatures (60, 70, 80, and 90 °C). The electrical characterization was performed by using an HP 4145B semiconductor parameter analyzer. The samples were measured in the dark, under ambient atmosphere, at room temperature.

**Supporting Information Available:** Tables of crystal data, structure refinement, atomic coordinates, bond lengths and angles, torsion angles, intermolecular contacts, and anisotropic thermal parameters for compounds **1** and **2** (14 pages); observed and calculated structure factors (40 pages). Ordering information is given on any current masthead page.

CM9804261